DOI: 10.1002/adma.200501875

Highly Raman-Enhancing Substrates Based on Silver Nanoparticle Arrays with Tunable Sub-10 nm Gaps**

By *Huai-Hsien Wang*, *Chih-Yu Liu*, *Shr-Bin Wu*, *Nai-Wei Liu*, *Cheng-Yi Peng*, *Tsu-Hsin Chan*, *Chen-Feng Hsu*, *Juen-Kai Wang*,* and *Yuh-Lin Wang**

Raman spectroscopy, which is based on the inelastic scattering of photons by chemical entities, has been successfully utilized for the investigation of adsorbed molecules on surfaces,[1–3] although the low cross section limits its applications. Surface-enhanced Raman scattering (SERS) has drawn a lot of attention since its discovery in 1974,[4] primarily because it can greatly enhance the normally weak Raman signal and thereby facilitate the convenient identification of the vibrational signatures of molecules in chemical and biological systems.[5] Recently, the observation of single-molecule Raman scattering has further enhanced the Raman detection sensitivity limit and widened the scope of SERS for sensor applications.[6,7]

Although SERS effects can be achieved simply by exploiting the electromagnetic resonance properties of roughened surfaces or nanoparticles of Au or Ag, the fabrication of reliable SERS substrates with uniformly high enhancement factors remains the focus of much research. Spraying Au or Ag colloids on a substrate leads to an extremely high SERS signal at some local 'hot-junctions';[6–8] however, it is not easy to achieve a reliable, stable, and uniform SERS signal spanning a wide dynamical range using this method. Van Duyne and co-workers have used nanosphere lithography,[9] while Liu and Lee exploited soft lithography,[10] in order to fabricate Ag nanoparticle arrays with high SERS activity and improved uniformity. Käll and co-workers have shown theoretically that the effective Raman cross section of a molecule placed between two metal nanoparticles can be enhanced by more than 12 orders of magnitude.[11] Such enhancement is likely to be related to the 'hot-junctions' observed in some SERS experiments. Several theoretical groups have also investigated field enhancement for SERS from metal nanoparticle arrays.[12–14] Specifically, García–Vidal and Pendry proposed that very localized plasmon modes, created by strong electromagnetic coupling between two adjacent metallic objects, dominate the SERS response in an array of nanostructures.[12] The interparticle-coupling-induced enhancement was attributed to the broadening of the plasmon resonance peak because the probability of the resonance covering both the excitation wavelength and the Raman peak increases with its width. They calculated the average enhancement factor over the surfaces of an array of infinitely long Ag nanorods with semicircular cross sections, and showed that significant near-field interaction occurs between adjacent nanorods when the gap between the nanorods reaches half the value of their diameter. Other groups have studied the dependence of the enhancement factor on the gap between adjacent nanoparticles on a SERS active substrate. For example, Gunnarsson et al. investigated SERS on ordered Ag nanoparticle arrays with an interparticle gap above 75 nm.[15] Lee and co-workers were able to achieve the temperature-controlled variation of interparticle gaps between Ag nanoparticles embedded in a polymer membrane.[16] Wei et al. performed SERS on self-organized Au nanoparticle arrays with narrow interparticle gaps,[17] although they have not carried out a detailed investigation of the dependence of the SERS signal on the interparticle gap. Sauer et al. investigated SERS from nanowire arrays embedded in an alumina matrix with interparticle gaps of ~110 nm, but no gap-related enhancement was observed in their experiment.[18] These theoretical and experimental studies indicate that the precise control of gaps between nanostructures on a SERS-active substrate in the sub-10 nm regime, which is extremely difficult to obtain by existing nanofabrication methods, is likely to be critical for the fabrication of substrates with uniformly high enhancement factors, and for understanding collective surface plasmons existing inside the gaps.

[*] Prof. Y.-L. Wang, Prof. J.-K. Wang, H.-H. Wang, C.-Y. Liu, S.-B. Wu, N.-W. Liu, C.-Y. Peng, T.-H. Chan, C.-F. Hsu
Institute of Atomic and Molecular Sciences, Academia Sinica
P.O. Box 23-166, Taipei 106 (Taiwan)
E-mail: ylwang@pub.iams.sinica.edu.tw
Prof. Y.-L. Wang, H.-H. Wang
Department of Physics, National Taiwan University
Taipei 106 (Taiwan)
Prof. J.-K. Wang
Center for Condensed Matter Sciences, National Taiwan University
Taipei 106 (Taiwan)
E-mail: jkwang@ccms.ntu.edu.tw
S.-B. Wu
Graduate Institute of Electro-Optical Engineering
National Taiwan University, Taipei 106 (Taiwan)
N.-W. Liu
Department of Materials Science and Engineering
National Taiwan University, Taipei 106 (Taiwan)

[**] We thank Dr. Y. F. Shieh of Ma-tek, Taiwan, for the TEM studies and Hsuan-Hao Chang for image processing. This work was supported by the National Science Council (Grant No. NSC 94-2120-M-001-002) and Academia Sinica, Taiwan.

© 2006 WILEY-VCH Verlag GmbH & Co. KGaA, Weinheim
WILEY InterScience DISCOVER SOMETHING GREAT

ADVANCED MATERIALS

In this report, we present SERS measurements of molecules adsorbed on arrays of Ag nanoparticles grown in porous anodic aluminum oxide (AAO) nanochannels with a precisely controlled variation of interparticle gaps between 5 and 25 nm.[18,19] Our results not only open new possibilities for applying SERS to different analytical measurements but also provide important information for improving the fundamental understanding of SERS phenomena.

Figures 1a–d schematically depict the procedure for fabricating arrays of Ag nanoparticles separated by tunable gaps on an AAO substrate with self-organized, hexagonally close-packed nanochannels. First, the AAO nanochannel substrate is fabricated by anodizing a finely polished aluminum foil. When required, the substrate is etched in 5 % phosphoric acid to widen the pore diameters (~ 1/2 of the channel spacing). By carefully controlling the etching time, arrays of nanochannels are obtained with a wall thickness of 5 ± 2 nm. This etching process allows us to fine tune the gap between the nanoparticles in an array, as the walls separate the Ag deposited into the nanochannels during the subsequent electrodeposition process, as illustrated in Figure 1d. After depositing Ag nanoparticles of the desired length, the upper part of the AAO film is etched away in phosphoric acid to increase the area of exposed Ag. The final geometry of the array of Ag nanoparticles partially embedded in an AAO substrate is shown schematically in Figure 1f, where *S*, *D*, and *W* are the interparticle spacing, particle diameter, and interparticle gap, respectively.

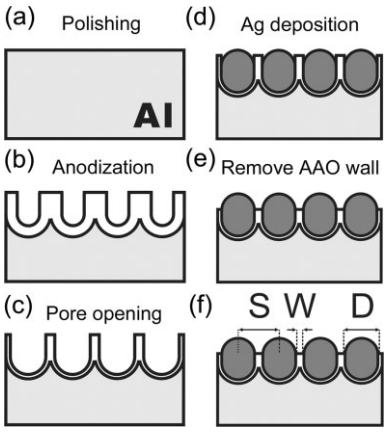

Figure 1. Schematic diagram showing the process for fabricating silver-filled porous anodic alumina substrates (see text for details).

Figures 2a,b show top-view images of a typical Ag/AAO substrate, whose pores have been widened to 25 nm by etching, before and after the growth of Ag nanoparticles, respectively. Images taken on a field emission scanning electron microscope (SEM) with a beam diameter of 1 nm (JEOL 6700) have been analyzed by using commercial software (Scanning Probe Image Processor, Image Metrology) to determine the distribution and spread of *D* and *W* for the nanoparticle array, as shown in Figures 2c,d, respectively. The size measurements are further confirmed by cross-sectional transmission electron microscopy (TEM) images, as exemplified by Figure 2e. The results indicate that it is possible to fabricate Ag nanoparticle arrays with a mean interparticle gap as small as 5 ± 2 nm. To further demonstrate the flexibility and precision of the fabrication process, Figure 2f shows the SEM image of a substrate with $D = 25$ nm, similar to Figure 2b, but with *W* widened to 15 nm.

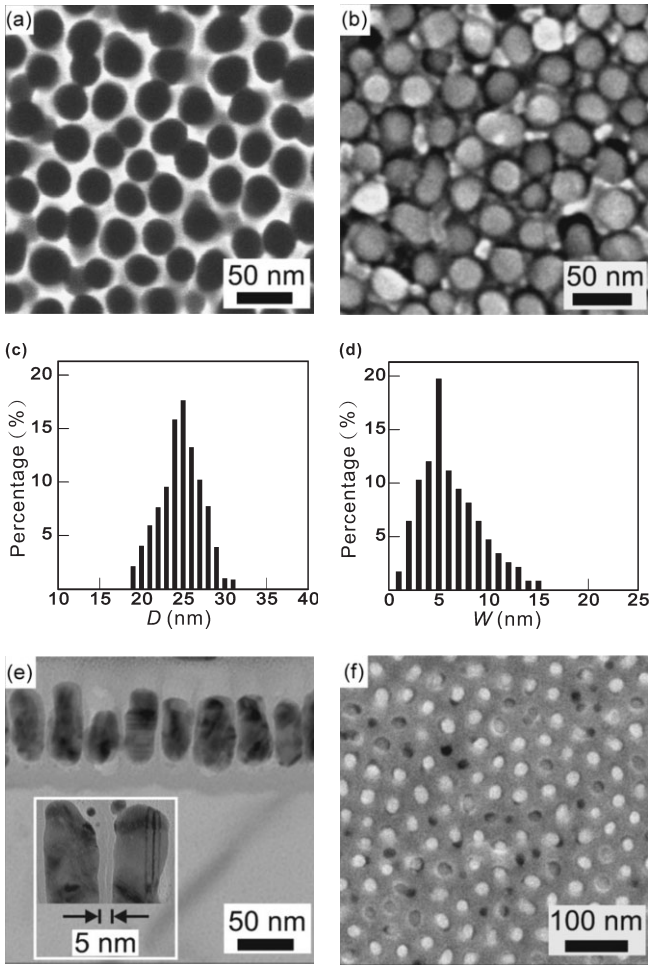

Figure 2. Top-view scanning electron microscopy (SEM) image of an AAO substrate with $D = 25$ nm and $W = 5$ nm, a) before and b) after growth of Ag nanoparticles. c,d) Histograms of *D* and *W*, respectively. e) TEM images of the Ag nanoparticles. f) SEM image of a substrate with $D = 25$ nm and $W = 15$ nm.

To test the Raman-enhancing capability of the Ag/AAO substrates, a water solution (10^{-6} M) of Rhodamine 6G (R6G) is applied to a substrate with $W = 5$ nm and $D = 25$ nm and the SERS spectrum is recorded. As shown in Figure 3a, high-intensity Raman peaks are observed when the fluorescence background is quenched to a steady state, a few minutes after the application of the solution, similar to some previous observations.[7,20] The large SERS signal indicates that the R6G molecules near the Ag nanoparticles are excited by the laser-induced surface plasmon, while the fluorescence quenching suggests that some of these molecules spontaneously adsorb

 © 2006 WILEY-VCH Verlag GmbH & Co. KGaA, Weinheim

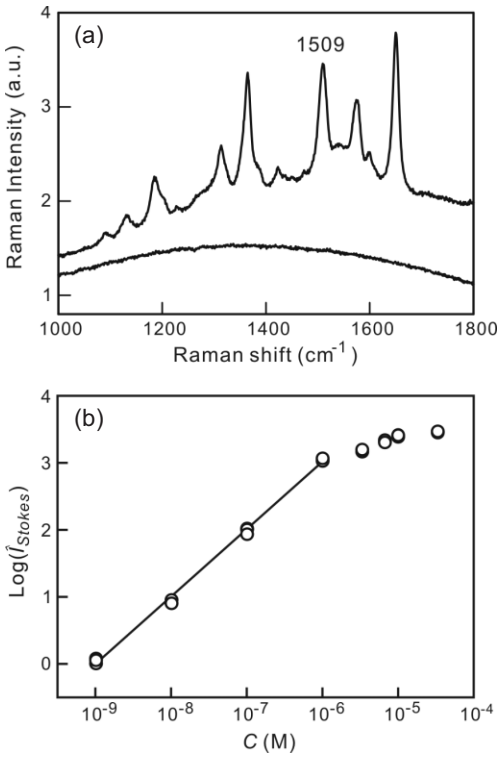

Figure 3. a) SERS spectrum of 10^{-6} M R6G solution on a Ag/AAO substrate with $W = 5$ nm and $D = 25$ nm (top), and on a typical SERS substrate prepared by depositing ~30 nm Ag on Si (bottom); b) SERS signal ($\log(\hat{I}_{Stokes})$) at 1509 cm^{-1} as a function of the molecular concentration on a logarithmic scale. The solid line is a guide to the eye.

onto the surface of the nanoparticles. The enhancement factor for the Ag/AAO substrate is at least 10^5 times larger than that of a SERS substrate prepared by depositing ~30 nm Ag onto a silicon surface, which does not provide a detectable SERS signal above the fluorescence background. The spectra are shown for comparison in Figure 3a. The strong enhancement can be attributed to the fact that the Ag/AAO substrate has a very high density of both Ag nanoparticles (~1×10^{11} cm^{-2}), and 'hot-junctions' (~3×10^{11} cm^{-2}), which likely exist in the gaps between neighboring nanoparticles, as will be discussed in more detail later. It is to be noted that the enhancing power is uniformly consistent over the entire 1 cm^2 sample with less than 5 % variation; further, the enhancing power is comparable (within the same order of magnitude) for different batches of substrates prepared by the same processing parameters, indicating the overall uniformity and reliability of the Ag/AAO substrates. In comparison with SERS substrates made from metallic colloids and roughened metal surfaces, the low variation of the enhanced Raman signal over various substrates further indicates that the molecular adsorption behavior and the chemical Raman enhancement effect in these Ag/AAO substrates are comparably insensitive to the fabrication procedure.

Solutions of R6G with different concentrations (6.7×10^{-5} to 10^{-9} M) have been used to study the SERS dynamical range of these Ag/AAO substrates. Figure 3b shows the Raman peak intensity (at 1509 cm^{-1}) versus the R6G concentration (C). The linear correlation from 10^{-6} to 10^{-9} M with a proportionality constant of unity suggests that the number of adsorption sites with high Raman enhancement is large enough to accommodate a considerable range of sample concentrations. A nonlinear dependence emerges for concentrations above 10^{-6} M, indicating that the adsorption of R6G onto adsorption sites with high enhancement becomes saturated beyond this level. In conjunction with the uniformly large enhancement factor obtained across the entire Ag/AAO substrate, the large dynamical range (more than three orders of magnitude) provides very clear justification for exploiting such nanofabricated substrates as platforms for the sensing of chemical and biological molecules by SERS.

A solution of adenine (10^{-4} M) in water has been used to probe the dependence of the Raman-enhancing power of the Ag/AAO substrates on the geometry of the Ag nanoparticle array, and to study the effect of the 'hot junctions' that are believed to exist between two nanoparticles separated by a gap of less than 10 nm. Adenine is chosen because it does not have any appreciable one-photon absorption at the excitation wavelength, and therefore has a very low fluorescence background, causing minimal interference with the SERS measurement. A typical SERS spectrum of adenine on Ag/AAO substrates, as shown in the inset of Figure 4a, has two prominent Raman peaks at 739 and 1330 cm^{-1}, corresponding to the purine ring breathing mode and the CN stretching mode, respectively.[21,22] As W is reduced below 25 nm with D fixed at 25 nm, the Raman peaks increase in intensity, slowly at first, then becoming significantly stronger at $W = 10$ nm, and finally showing a dramatic enhancement when W reaches an unprecedented value of 5 nm, as demonstrated by the dependence of the integrated intensity of the 739 cm^{-1} peak on W (Fig. 4a). The dramatic enhancement observed at $W = 5$ nm is again likely to be the result of the high density of Ag nanoparticles and 'hot junctions' on the Ag/AAO substrate.

In order to evaluate the dependence of the enhancement factor of the substrate on W, it is better to rescale the relative Raman signal according to the number of Ag nanoparticles that are illuminated by the laser. Figure 4b shows $\hat{I}_{Stokes}/\hat{I}^{\infty}_{Stokes}$ as a function of the gap-to-diameter ratio (W/D), in which $\hat{I}_{Stokes}$ is the average Raman signal per Ag nanoparticle and $\hat{I}^{\infty}_{Stokes}$ is $\hat{I}_{Stokes}$ for substrates with a large W. When compared with predictions made by García–Vidal and Pendry, our experiment shows a similar threshold behavior.[12] The theoretical calculations appear to be more sensitive to variations in W/D. We believe that this discrepancy possibly arises from the fact that the calculation was based on an array of infinitely long, semicircular Ag nanorods instead of a two-dimensional (2D) array of Ag nanoparticles arranged on the substrate in a specific geometry, as used in our experiment. The experimental data seem to match very nicely with the predictions made in the theoretical study performed by Xu and Dignam on the dependence of the SERS signal on the gap between Ag nanoparticles ($D = 10$ nm) arranged in a linear chain, using a full-

 © 2006 WILEY-VCH Verlag GmbH & Co. KGaA, Weinheim

ADVANCED MATERIALS

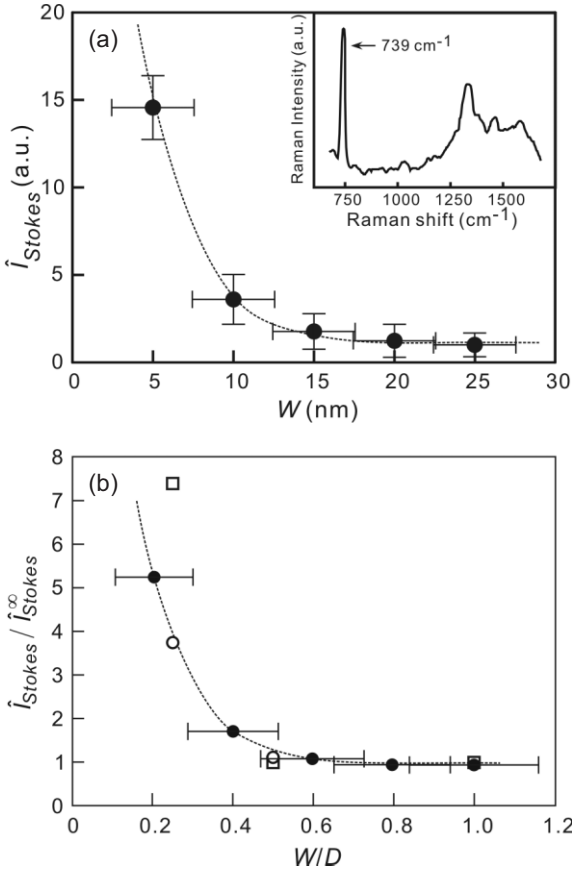

Figure 4. a) Integrated Raman intensity of adenine at 739 cm^{-1} as a function of the interparticle gap width (W) for different Ag/AAO substrates. $\hat{I}_{Stokes}$ is the average Raman signal per Ag particle and $\hat{I}^{\infty}_{Stokes}$ is $\hat{I}_{Stokes}$ for a large interparticle gap width. The inset shows a typical SERS spectrum of adenine. b) Comparison between the normalized SERS signal as a function of W/D from our results (filled circles) and theoretical predictions (average normalized Raman enhancement factor) by Xu and Dignam [23] (open circles) and by García–Vidal and Pendry [12] (open squares). The dashed lines are guides to the eye.

scale analytic solution.[23] Given the differences between the theory and experiment in tems of the size of the Ag nanoparticles and the geometry of the array, the remarkable match shown in Figure 4b suggests that the threshold behavior of the enhancement factor depends primarily on the W/D ratio.

Based on SERS measurements of thiophenol adsorbed on Si substrates covered by arrays of 200 nm Ag nanoparticles with W varying over a very large scale, between 75 and 270 nm,[15] Käll and co-workers pointed out that for interparticle coupling effects on Raman scattering, the light field needs to be perpendicular to the metal surface. Giese and McNaughton[21] and Watanabe et al.[22] have shown both theoretically and experimentally that adenine adsorbs essentially perpendicular to the Ag surface. The purine ring breathing mode of adenine at 739 cm^{-1} observed in our experiment is therefore essentially parallel to the interparticle axis, which allows us to attribute its efficient Raman scattering to the coupling of plasmons in the array of Ag nanoparticles with extremely small W. It is worth mentioning that the dependence of the enhancement factor on W/D reported by Käll and coworkers is noticeably different from our result.[15] This difference could originate from the much larger D and W of their arrays and from the disk-like shape of their Ag nanoparticles. These geometric factors can produce distinct local field distributions between nanoparticles and therefore lead to different interparticle interactions. Su et al. have suggested that the peak position of the plasmon resonance for an array of metallic nanoparticles with a given W/D depends sensitively on the shape of the nanoparticles.[24]

In conclusion, we have presented a SERS-active substrate made of an array of Ag nanoparticles partially embedded in AAO with nanochannels. This substrate exhibits an ultrahigh Raman signal enhancement factor due to the unprecedented narrow gaps between the Ag nanoparticles. This experiment represents the first quantitative observation of the collective SERS effect on a substrate with precisely controlled 'hot junctions' in the sub-10 nm regime, and confirms the theoretical prediction of interparticle-coupling-induced Raman enhancement. The uniform and highly reproducible SERS-active properties obtained for the Ag/AAO substrate and its wide dynamical range will facilitate the use of SERS for chemical/biological sensing applications with extremely high sensitivity. The substrate can be further improved by fabricating long-range ordered arrays and/or by using custom-designed anodic nanochannels made by focused ion beam lithographic guiding techniques.[25–28]

Experimental

High-purity (99.99 %) annealed aluminum foil was electropolished in a mixture of $HClO_4$ and C_2H_5OH (volume ratio 1:5) until the root-mean-square surface roughness of a typical 10 μm × 10 μm area was 1 nm, as measured using an atomic force microscope operating in contact mode. The foil was then anodized in sulfuric acid (0.3 M) at 5 °C using a voltage in the 10–30 V range to obtain AAO substrates with arrays of self-organized nanochannels with the specific pore diameters and spacings required for this study. For growing Ag nanoparticles in the AAO nanochannels, an alternating current (AC) (9 V) electrochemical plating procedure was employed using a mixture of silver nitrate (0.006 M) and magnesium sulfate (0.165 M) as the electrolyte solution with a pH value of 2, set by the addition of sulfuric acid. Since the deposition of Ag occurred primarily inside the nanochannels, it was possible to avoid the merging of Ag nanoparticles by confining them inside the channels.

Raman spectroscopy measurements were performed on a micro-Raman setup with an argon-ion laser at 514.5 nm. After passing through a narrow bandpass filter to remove residual plasma lines, the laser beam was focused by a 100× water-immersion objective lens (numerical aperture (NA) = 0.95) to a ~1 μm spot on a drop of the desired solution on a Ag/AAO substrate with a resultant beam intensity of ~ 10^5 W cm^{-2}. The scattered radiation was collected by the same objective lens and sent through a Raman notch filter to a 64 cm monochromator. The dispersed spectrum was then detected by a liquid-N_2-cooled charge-coupled device (CCD) camera. The low laser power density used for the measurements prevented adverse side effects, such as local heating, deformation of Ag nanoparticles, and photooxidation, from occurring during laser illumination.

Received: September 6, 2005
Final version: October 26, 2005

 © 2006 WILEY-VCH Verlag GmbH & Co. KGaA, Weinheim

[1] W. Suëtaka, *Surface Infrared and Raman Spectroscopy*: *Methods and Applications*, Plenum, New York **1995**, Ch. 5.
[2] C. S. Tsai, C. Chen, C. E. Lin, J. C. Lin, J. K. Wang, *Surf. Sci.* **1999**, *318*, 427.
[3] J. K. Wang, C. S. Tsai, C. E. Lin, J.-C. Lin, *J. Chem. Phys.* **2000**, *113*, 5041.
[4] M. Fleischmann, P. J. Hendra, A. McQuillan, *Chem. Phys. Lett.* **1974**, *26*, 163.
[5] A. Campion, P. Kambhampati, *Chem. Soc. Rev.* **1998**, *4*, 241.
[6] K. Kneipp, Y. Wang, H. Kneipp, L. T. Perelman, I. Itzkan, R. R. Dasari, M. S. Feld, *Phys. Rev. Lett.* **1996**, *78*, 1667.
[7] S. Nie, S. R. Emory, *Science* **1997**, *275*, 1102.
[8] H. Xu, E. J. Bjerneld, M. Käll, L. Börjesson, *Phys. Rev. Lett.* **1999**, *83*, 4357.
[9] a) C. L. Hynes, R. P. Van Duyne, *J. Phys. Chem. B* **2003**, *107*, 7426. b) T. R. Jensen, G. C. Schatz, R. P. Van Duyne, *J. Phys. Chem. B* **1999**, *103*, 2394.
[10] G. L. Liu, L. P. Lee, *Appl. Phys. Lett.* **2005**, *87*, 074 101.
[11] H. Xu, J. Aizpurua, M. Käll, P. Apell, *Phys. Rev. E* **2000**, *62*, 4318.
[12] F. J. García-Vidal, J. B. Pendry, *Phys. Rev. Lett.* **1996**, *77*, 1163.
[13] M. Kahl, E. Voges, *Phys. Rev. B: Condens. Matter* **2000**, *61*, 14 078.
[14] D. A. Genov, A. K. Sarychev, V. M. Shalaev, A. Wei, *Nano Lett.* **2004**, *4*, 153.
[15] L. Gunnarsson, E. J. Bjerneld, H. Xu, S. Petronis, B. Kasemo, M. Käll, *Appl. Phys. Lett.* **2001**, *78*, 802.
[16] Y. Lu, G. L. Liu, L. P. Lee, *Nano Lett.* **2005**, *5*, 5.
[17] A. Wei, B. Kim, B. Sadtler, S. L. Tripp, *ChemPhysChem* **2001**, *2*, 743.
[18] G. Sauer, G. Brehm, S. Schneider, H. Graener, G. Seifert, K. Nielsch, J. Choi, P. Göring, U. Gösele, P. Miclea, R. B. Wehrspohn, *J. Appl. Phys.* **2005**, *97*, 024 308.
[19] F. Li, L. Zhang, R. M. Metzger, *Chem. Mater.* **1998**, *10*, 2470.
[20] J. Jiang, K. Bosnick, M. Maillard, L. Brus, *J. Phys. Chem. B* **2003**, *107*, 9964.
[21] B. Giese, D. J. McNaughton, *J. Phys. Chem. B* **2002**, *106*, 101.
[22] H. Watanabe, Y. Ishida, N. Hayazawa, Y. Inouye, S. Kawata, *Phys. Rev. B: Condens. Matter* **2004**, *69*, 155 418.
[23] M. Xu, M. J. Dignam, *J. Chem. Phys.* **1994**, *100*, 197.
[24] K. H. Su, Q. H. Wei, X. Zhang, J. J. Mock, D. R. Smith, S. Schultz, *Proc. SPIE—Int. Soc. Opt. Eng.* **2003**, *5221*, 108.
[25] C. Y. Liu, A. Datta, Y. L. Wang, *Appl. Phys. Lett.* **2001**, *78*, 120.
[26] C. Y. Liu, A. Datta, N. W. Liu, C. Y. Peng, Y. L. Wang, *Appl. Phys. Lett.* **2004**, *84*, 2509.
[27] N. W. Liu, A. Datta, C. Y. Liu, C. Y. Peng, H. H. Wang, Y. L. Wang, *Adv. Mater.* **2005**, *17*, 222.
[28] C. Y. Peng, C. Y. Liu, N. W. Liu, H. H. Wang, A. Datta, Y. L. Wang, *J. Vac. Sci. Technol. B* **2005**, *23*, 559.

 © 2006 WILEY-VCH Verlag GmbH & Co. KGaA, Weinheim